

Acoustic Source Localization in Shallow Water: A Probabilistic Focalization Approach

Florian Meyer* and Kay L. Gemba†

*Scripps Institution of Oceanography and Department of Electrical and Computer Engineering
University of California San Diego, La Jolla, CA (flmeyer@ucsd.edu)

†Physics Department, Naval Postgraduate School, Monterey, California 93943, USA (kgemba@nps.edu)

Abstract—This paper presents a Bayesian estimation method for the passive localization of an acoustic source in shallow water. Our probabilistic focalization approach estimates the time-varying source location by associating direction of arrival (DOA) observations to DOAs predicted based on a statistical model. Embedded ray tracing makes it possible to incorporate environmental parameters and characterize the nonlinear acoustic waveguide. We demonstrate performance advantages of our approach compared to matched field processing using data collected during the *SWellEx-96* experiment.

Index Terms—Array processing, data association, direction of arrival (DOA) estimation, source localization, ray tracing.

I. INTRODUCTION

In the shallow water environment, knowledge of the acoustic waveguide can be used to exploit multipath propagation for source localization. In particular, it has been demonstrated that a typical shallow water waveguide offers sufficient coherence times and ray-path diversity (or aperture) to determine the range and depth of an acoustic source from the measurements provided by a single vertical line array (VLA) [1].

A. State-of-the-Art

Matched field processing [2]–[4] (MFP) is a scientific approach to shallow water localization that compares modeled signal replicas with acoustic data in order to determine the location of one or multiple sources. A potential limitation of MFP is the fact that modeling the channel between a candidate source position and a VLA requires detailed knowledge of environmental parameters.

MFP is still an active research topic [5]–[10] because in real-world scenarios, knowledge of the acoustic environment, in particular an accurate model of the seabed, is typically unavailable. Recent approaches to shallow water localization explicitly consider environmental uncertainty to offer a degree of robustness to model mismatch [8], [11], [12].

B. Contribution and Paper Organization

This paper presents an innovative approach for the localization and tracking of an underwater source with a probabilistic model of the environment. Signals transmitted by an acoustic source are received by a VLA. Inspired by recently proposed graph-based methods for multitarget tracking and indoor localization and mapping [13]–[18], the proposed sequential probabilistic focalization [19] method associates direction of arrival

(DOA) observations to modeled DOAs and jointly estimates the time-varying position of the source. Embedded ray tracing makes it possible to incorporate environmental parameters such as the SSP (sound speed profile) of the acoustic channel. Evaluation of the proposed method is performed based on acoustic data from the *SWellEx-96* shallow water localization scenario shown in Fig. 1. The contributions of this paper are as follows.

- We introduce a new probabilistic model for the localization of an acoustic source in the shallow water waveguide by using a VLA.
- We establish a Bayesian estimation method based on the new model and evaluate its performance using data collected during the *SWellEx-96* experiment.

An important aspect is the *probabilistic data association* of DOA observations to modeled propagation paths for a source and VLA geometry. The considered model calculates expected DOAs by means of ray tracing based on the SSP and, if available, a characterization of the seabed.

II. SYSTEM MODEL

We consider a mobile source with unknown time-varying position $\mathbf{p}_n \in \mathbb{R}^2$ which, due to the azimuthal ambiguity of DOA information provided by the VLA, only consists of range and depth. There are K propagation paths that are used for localization. In each discrete time slot n , the array acts as a receiver and provides DOA observations. A DOA estimation method [20], [21] processes the acoustic signals received by the VLA and returns M_n DOA estimates at time n . M_n at time n is related to the number of propagation paths K as follows: It is possible that some propagation paths are not “detected” by the DOA estimator and thus do not generate a DOA estimate, and it is also possible that some DOA estimates do not correspond to a propagation path. Accordingly, M_n may be smaller than, equal to, or larger than K . Note also that M_n depends on the source position \mathbf{p}_n and on the environment. Selecting the number of propagation paths K requires some a priori understanding of the propagation environment.

A. Source State and Association Vectors

The state of the source at time n is $\mathbf{x}_n \triangleq [\mathbf{p}_n^T \ v_n]^T$, where v_n is the source speed in range. The source state \mathbf{x}_n is assumed to evolve according to Markovian state dynamics,

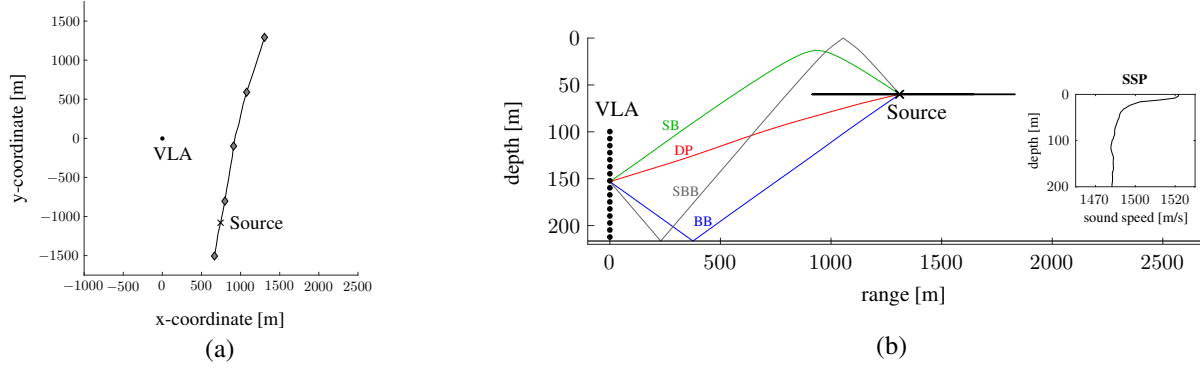


Fig. 1. Considered shallow water localization scenario from the *SWellEx-96* experiment with VLA position and source track in the time interval 11-May-1996 00:05:00–00:25:00 UTC. (a) shows the track of the acoustic source towed by the R/V Sprout at a depth of roughly 60m. The black cross shows the source position at time 00:08:00 UTC and gray diamonds indicate source positions in 5 minutes intervals. (b) shows the VLA and source track in range and depth. The black cross indicates the same source position as in (a). The $K = 4$ dominant propagation paths **direct path (DP)**, **surface bounce (SB)**, **bottom bounce (BB)**, and **surface-bottom bounce (SBB)**, are shown.

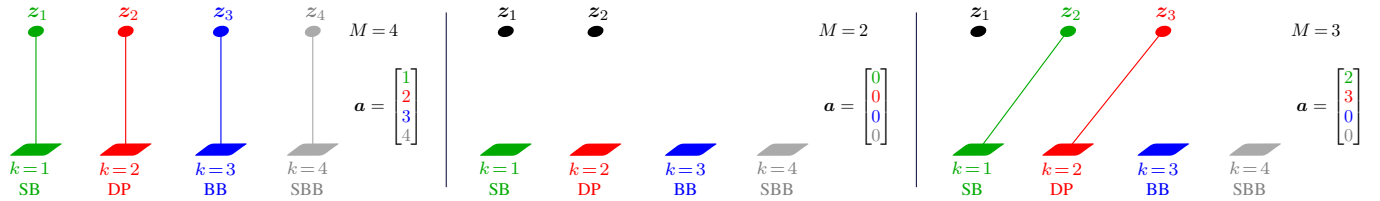


Fig. 2. Three example realizations of DOA observations $\mathbf{z}_n \triangleq [z_{1,n}^T \cdots z_{M,n}^T]^T$ and data association vector \mathbf{a}_n for the scenario Fig. 1. Associations of DOA observations to the $K = 4$ modeled propagation paths **surface bounce (SB)**, **direct path (DP)**, **bottom bounce (BB)**, and **surface-bottom bounce (SBB)**, are shown. The time index n is omitted.

where $f(\mathbf{x}_n|\mathbf{x}_{n-1})$ is the state-transition probability density function (PDF) of the source state. At time $n = 0$, the source state \mathbf{x}_0 is distributed according to a uninformative prior PDF $f(\mathbf{x}_0)$.

The DOA observations $z_{m,n} \in [-90^\circ, 90^\circ)$, $m \in \{1, \dots, M_n\}$ are subject to observation-origin uncertainty. That is, it is not known which observation $z_{m,n}$ is associated with which propagation path $\{1, \dots, K\}$, or if an observation $z_{m,n}$ did not originate from any propagation path (this is known as a *false alarm*), or if a propagation path did not give rise to any observation (this is known as a *missed detection*). The probability that a propagation path is “detected” in the sense that it generates an observation $z_{m,n}$ in the DOA estimation stage is denoted by $d_k(\mathbf{p}_n) \in [0, 1]$. (For positions \mathbf{p}_n for which a propagation path k is geometrically impossible, we set $d_k(\mathbf{p}_n) = 0$.) False alarms are independent and identically distributed as $f_{\text{FA}}(z_{m,n})$. The number of false alarms is assumed Poisson distributed with mean μ_{FA} [13], [14], [22]. $f_{\text{FA}}(z_{m,n})$, and μ_{FA} are known. The DOA observations resulting from propagation paths that are not modeled among the K selected paths are treated as false alarms. Finally, we introduce the total observation vector $\mathbf{z}_n \triangleq [z_{1,n} \cdots z_{M_n,n}]^T$ that is assumed sorted in descending order, i.e., $z_{m,n} \geq z_{m+1,n}$, $m \in \{1, \dots, M_n - 1\}$.

The associations between DOA observation $m \in$

$\{1, \dots, M_n\}$ and propagation path $k \in \{1, \dots, K\}$ at time n can be described by the K -dimensional *data association vector* $\mathbf{a}_n = [a_{1,n} \cdots a_{K,n}]^T$, whose k th entry is given by $a_{k,n} = m \in \{1, \dots, M_n\}$ if propagation path k generates observation $z_{m,n}$, and $a_{k,n} = 0$ if it does not generate any observation. Due to observation-origin uncertainty, \mathbf{a}_n is a random variable. However, since the DOAs of the propagation paths have a fixed order [23] and each propagation path can generate at most one DOA observation [13], [14], [22] at any time n , only certain data association vectors \mathbf{a}_n are valid. To facilitate identifying invalid vectors \mathbf{a}_n , we order its elements $a_{1,n}, \dots, a_{K,n}$ such that for the case where there are no false alarms and no missed detections, we have $\mathbf{z}_n = [z_{a_{1,n},n} \cdots z_{a_{K,n},n}]^T$. With this order a general association vector \mathbf{a}_n is invalid if and only if there exist $k, k' \in \{1, \dots, K\}$ with $k > k'$ such that $a_{k',n} \geq a_{k,n} \neq 0$.

For examples, let us assume that we use the $K = 4$ propagation paths shown in Fig. 1. According to the order defined above, we have $k = 1$ for the SB, $k = 2$ for the DP, $k = 3$ for the BB, and $k = 4$ for the SBB. It can easily be verified that for the case where there is a measurement for each propagation path and no false alarm, we obtain $a_{1,n} = 1$, $a_{2,n} = 2$, $a_{3,n} = 3$, and $a_{4,n} = 4$ as well as $z_{1,n} \geq z_{2,n} \geq z_{3,n} \geq z_{4,n}$ (cf. with the DOAs of the four propagation paths at the VLA shown in Fig. 1).

B. Observation Model

At each time step n , a DOA estimation method [20], [21] provides DOAs $z_{m,n}$, $m \in \{1, \dots, M_n\}$. These DOAs are considered as the observations in our statistical model. Let $z_{m,n}$ be the DOA observations related to propagation path $k \in \{1, \dots, K\}$. The observation model is then given by

$$z_{m,n} = g_k(\mathbf{p}_n) + w_{k,n}. \quad (1)$$

Here, $w_{k,n}$ is zero mean Gaussian distributed with variance σ_k^2 and $g_k(\mathbf{p}_n)$ is the DOA of propagation path k . The observation noise $w_{k,n}$ assumed statistical independent across time n and propagation path k . From (1), we directly get the conditional PDF $f_k(z_{m,n}|\mathbf{x}_n)$. The functions $g_k(\mathbf{p}_n)$ are the DOAs of eigenrays related to the considered propagation paths. The eigenrays are obtained using the BELLHOP [24] ray-tracing software that can incorporate the SSP and a model of the seabed. Details on how the $g_k(\mathbf{p}_n)$, $k \in \{1, \dots, K\}$ can be precomputed offline will be discussed in Section IV.

C. Measurement Model

The conditional PDFs $f_k(z_{m,n}|\mathbf{x}_n)$ obtained from (1) characterize the statistical relation between the observations $z_{m,n}$ and the states \mathbf{x}_n . This PDF is a central element in the conditional PDF of the total observation vector \mathbf{z}_n given \mathbf{x}_n , \mathbf{a}_n , and M_n . Let us introduce the set of detected paths at time n as $\mathcal{D}_{\mathbf{a}_n} \triangleq \{k \in \{1, \dots, K\} | a_{k,n} \neq 0\}$. Conditioned on \mathbf{x}_n , we assume that DOAs generated by the source are statistical independent of false alarms, i.e., we can write

$$f(\mathbf{z}_n | \mathbf{x}_n, \mathbf{a}_n, M_n) = \left(\prod_{m=1}^{M_n} f_{\text{FA}}(z_{m,n}) \right) \left(\prod_{k \in \mathcal{D}_{\mathbf{a}_n}} \frac{f_k(z_{a_{k,n},n} | \mathbf{x}_n)}{f_{\text{FA}}(z_{a_{k,n},n})} \right) \quad (2)$$

if the number of elements in the vector \mathbf{z}_n is equal to M_n and $f(\mathbf{z}_n | \mathbf{x}_n, \mathbf{a}_n, M_n) = 0$, otherwise. For example, let us again assume $K = 4$ and discuss three example realizations of M_n and \mathbf{a}_n . These three example realizations are shown in Fig. 2. In the ideal case where there is no missed detection and no false alarm, i.e., $M_n = 4$ and $\mathbf{a}_n = [1 \ 2 \ 3 \ 4]^T$, the conditional PDF in (2) reads $f(\mathbf{z}_n | \mathbf{x}_n, \mathbf{a}_n, M_n) = \prod_{k=1}^4 f_k(z_{k,n} | \mathbf{x}_n)$. Similarly, in case there is no detected path and two false alarms, i.e., $M_n = 2$ and $\mathbf{a}_n = [0 \ 0 \ 0 \ 0]^T$, we have $f(\mathbf{z}_n | \mathbf{x}_n, \mathbf{a}_n, M_n) = \prod_{m=1}^2 f_{\text{FA}}(z_{m,n})$. Finally, if we only detect the DP and the SB and there is also one missed detection, e.g., $M_n = 3$ and $\mathbf{a}_n = [2 \ 3 \ 0 \ 0]^T$, we have $f(\mathbf{z}_n | \mathbf{x}_n, \mathbf{a}_n, M_n) = f_{\text{FA}}(z_{1,n}) f_1(z_{2,n} | \mathbf{x}_n) f_2(z_{3,n} | \mathbf{x}_n)$.

Let us consider $f(\mathbf{z}_n | \mathbf{x}_n, \mathbf{a}_n, M_n)$ as a *likelihood function*, i.e., a function of \mathbf{x}_n , \mathbf{a}_n , and M_n , for observed \mathbf{z}_n . If \mathbf{z}_n is observed and therefore fixed, also M_n is fixed, and we can rewrite (2), up to a constant normalization factor, as

$$f(\mathbf{z}_n | \mathbf{x}_n, \mathbf{a}_n, M_n) \propto \prod_{k=1}^K h_k(\mathbf{x}_n, a_{k,n}; \mathbf{z}_n).$$

Here, the factors $h_k(\mathbf{x}_n, a_{k,n}; \mathbf{z}_n)$ are defined as

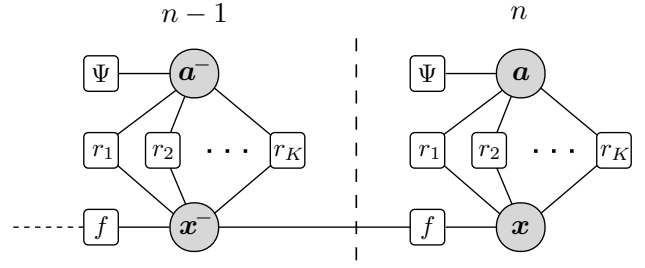


Fig. 3. Factor graph representing the factorization of the joint posterior PDF $f(\mathbf{x}_{1:n}, \mathbf{a}_{1:n} | \mathbf{z}_{1:n})$ in (7) depicted for two time steps $n' \in \{n-1, n\}$. The time index is omitted and the following short notations are used: $f \triangleq f(\mathbf{x}_{n'} | \mathbf{x}_{n'-1})$, $r_k \triangleq r_k(\mathbf{x}_{n'}, a_{k,n'}; \mathbf{z}_{n'})$, $\mathbf{x} \triangleq \mathbf{x}_n$, $\mathbf{a} \triangleq \mathbf{a}_n$, $\mathbf{x}^- \triangleq \mathbf{x}_{n-1}$, and $\mathbf{a}^- \triangleq \mathbf{a}_{n-1}$.

$$h_k(\mathbf{x}_n, a_{k,n}; \mathbf{z}_n) \triangleq \begin{cases} \frac{f_k(z_{a_{k,n},n} | \mathbf{x}_n)}{f_{\text{FA}}(z_{a_{k,n},n})}, & a_{k,n} \in \{1, \dots, M_n\} \\ 1, & a_{k,n} = 0. \end{cases}$$

Finally, the likelihood function for $\mathbf{z}_{1:n} \triangleq [\mathbf{z}_1^T \dots \mathbf{z}_n^T]^T$, involving the observations $z_{m,n'}$ of all time steps $n' = 1, \dots, n$, is obtained as

$$f(\mathbf{z}_{1:n} | \mathbf{x}_{1:n}, \mathbf{a}_{1:n}, \mathbf{m}_{1:n}) = \prod_{n'=1}^n f(\mathbf{z}_{n'} | \mathbf{x}_{n'}, \mathbf{a}_{n'}, M_{n'}) \quad (3)$$

where we introduced $\mathbf{m}_n = [M_1 \dots M_n]^T$. (Recall that M_n is the number of detected DOAs at time n .)

D. Prior Information

Now, one can derive [14], [22] the following expression of the joint conditional prior probability mass function (pmf) of the data association vector \mathbf{a}_n , and the number of observations M_n , conditioned on the state \mathbf{x}_n of the mobile source,

$$p(\mathbf{a}_n, M_n | \mathbf{x}_n) = \frac{e^{-\mu_{\text{FA}}} \mu_{\text{FA}}^{M_n - |\mathcal{D}_{\mathbf{a}_n}|} |\mathcal{D}_{\mathbf{a}_n}|!}{M_n!} \left(\prod_{k \in \mathcal{D}_{\mathbf{a}_n}} d_k(\mathbf{p}_n) \right) \times \psi(\mathbf{a}_n) \prod_{k' \notin \mathcal{D}_{\mathbf{a}_n}} (1 - d_{k'}(\mathbf{p}_n)). \quad (4)$$

Here, $\psi(\mathbf{a}_n)$ checks the validity of association vector \mathbf{a}_n as discussed in Section II-A. In particular, it is defined to be 0 if there exist $k, k' \in \{1, \dots, K\}$ with $k > k'$ such that $a_{k',n} \geq a_{k,n} \neq 0$, and to be 1 otherwise. The function $\psi(\mathbf{a}_n)$ enforces $p(\mathbf{a}_n, M_n | \mathbf{x}_n) = 0$ if any observation is associated with more than one propagation path. For future reference, we can also express (4) as

$$p(\mathbf{a}_n, M_n | \mathbf{x}_n) \propto C(M_n) \psi(\mathbf{a}_n) \prod_{k=1}^K v(\mathbf{x}_n, a_{k,n}; M_n)$$

where the factors $v(\mathbf{x}_n, a_{k,n}; M_n)$ are defined as

$$v(\mathbf{x}_n, a_{k,n}; M_n) \triangleq \begin{cases} \frac{d_k(\mathbf{p}_n)}{\mu_{\text{FA}}} & a_{k,n} \in \{1, \dots, M_n\} \\ 1 - d_k(\mathbf{p}_n), & a_{k,n} = 0. \end{cases}$$

and $C(M_n) = e^{-\mu_{\text{FA}}} \mu_{\text{FA}}^{M_n} |\mathcal{D}_{\mathbf{a}_n}|! / M_n!$.

Using common assumptions [13], [14], [22], the joint prior distribution for all source states, association variables, and number of observations up to time n , is given by

$$\begin{aligned} f(\mathbf{x}_{1:n}, \mathbf{a}_{1:n}, \mathbf{m}_{1:n}) \\ = f(\mathbf{x}_0) \prod_{n'=1}^n p(\mathbf{a}_{n'}, M_{n'} | \mathbf{x}_{n'}) f(\mathbf{x}_{n'} | \mathbf{x}_{n'-1}). \end{aligned} \quad (5)$$

III. PROBLEM FORMULATION AND ESTIMATION

At time n , our goal is to estimate the source state \mathbf{x}_n from the total observation vector $\mathbf{z}_{1:n}$. For estimating \mathbf{x}_n , we will develop an approximate calculation of the minimum mean-square error (MMSE) estimator [25]

$$\hat{\mathbf{x}}_n^{\text{MMSE}} \triangleq \int \mathbf{x}_n f(\mathbf{x}_n | \mathbf{z}_{1:n}) d\mathbf{x}_n. \quad (6)$$

This estimator involves the posterior PDF $f(\mathbf{x}_n | \mathbf{z}_{1:n})$ which is a marginal of the joint posterior PDF $f(\mathbf{x}_{1:n}, \mathbf{a}_{1:n} | \mathbf{z}_{1:n})$ and involves all the source states, all the association variables, and all the observations, at all times up to the current time n .

In the following derivation of the factorization of $f(\mathbf{x}_{1:n}, \mathbf{a}_{1:n} | \mathbf{z}_{1:n})$, the observations $\mathbf{z}_{1:n}$ are considered observed and thus fixed, and consequently the numbers of observations $\mathbf{m}_{1:n}$ are fixed as well. Then, using Bayes' rule and the fact that $\mathbf{z}_{1:n}$ implies $\mathbf{m}_{1:n}$, we obtain

$$\begin{aligned} f(\mathbf{x}_{1:n}, \mathbf{a}_{1:n} | \mathbf{z}_{1:n}) \\ = f(\mathbf{x}_{1:n}, \mathbf{a}_{1:n}, \mathbf{m}_{1:n} | \mathbf{z}_{1:n}) \\ \propto f(\mathbf{z}_{1:n} | \mathbf{x}_{1:n}, \mathbf{a}_{1:n}, \mathbf{m}_{1:n}) f(\mathbf{x}_{1:n}, \mathbf{a}_{1:n}, \mathbf{m}_{1:n}). \end{aligned}$$

Inserting (5) for $f(\mathbf{x}_{1:n}, \mathbf{a}_{1:n}, \mathbf{m}_{1:n})$ and (3) for $f(\mathbf{z}_{1:n} | \mathbf{x}_{1:n}, \mathbf{a}_{1:n}, \mathbf{m}_{1:n})$, then yields the final factorization

$$\begin{aligned} f(\mathbf{x}_{1:n}, \mathbf{a}_{1:n} | \mathbf{z}_{1:n}) \propto f(\mathbf{x}_0) \prod_{n'=1}^n \Psi(\mathbf{a}_{n'}) f(\mathbf{x}_{n'} | \mathbf{x}_{n'-1}) \\ \times \prod_{k=1}^K r_k(\mathbf{x}_{n'}, a_{k,n'}; \mathbf{z}_{n'}) \end{aligned} \quad (7)$$

with

$$r_k(\mathbf{x}_n, a_{k,n}; \mathbf{z}_n) \triangleq v(\mathbf{x}_n, a_{k,n}; M_n) h_k(\mathbf{x}_n, a_{k,n}; \mathbf{z}_n)$$

and $\Psi(\mathbf{a}_n) \triangleq |\mathcal{D}_{\mathbf{a}_n}|! \psi(\mathbf{a}_n)$. The factor graph representing this factorization of the joint posterior PDF is depicted for one time step in Fig. 3. By applying the sum-product algorithm (SPA) [26] on this factor graph, accurate approximations (“beliefs”) $f(\mathbf{x}_n | \mathbf{z}_{1:n})$ of the marginal posterior PDFs $f(\mathbf{x}_n | \mathbf{z}_{1:n})$, used for estimation in (6), are obtained in an efficient way.

In order to obtain accurate nonlinear estimation by means of the SPA, we represent messages related to continuous state variables by random samples or particles [13], [27]. Thus, our algorithm produces a particle representation $\{(\mathbf{x}_n^{(j)}, \omega_n^{(j)})\}_{j=1}^J$ of the posterior PDF $f(\mathbf{x}_n | \mathbf{z}_{1:n})$ at each time step n , i.e., a particle-based approximation of the posterior $f(\mathbf{x}_n | \mathbf{z}_{1:n})$ is

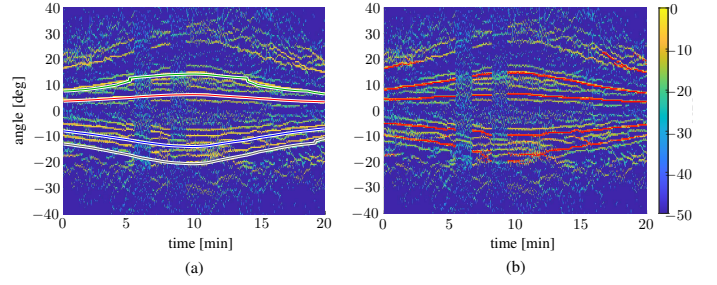


Fig. 4. DOA measurements obtained by multi-frequency sparse Bayesian learning versus time and corresponding modeled DOAs. In (a) the expected DOAs related to the four dominant propagation paths are overlaid. These DOAs are obtained by using a source range calculated from the global positioning system (GPS) system of the R/V Sproul, a reference depth of 60 m, and by applying the considered propagation model, respectively. In Fig. 4(b), the DOA estimates used as observations by the proposed method are highlighted in red.

given by $\tilde{f}(\mathbf{x}_n | \mathbf{z}_{1:n}) = \sum_{j=1}^J \omega_n^{(j)} \delta(\mathbf{x}_n - \mathbf{x}_n^{(j)})$. An approximation of the estimate $\hat{\mathbf{x}}_n^{\text{MMSE}}$ in (6) is then obtained from the respective particle representation as

$$\hat{\mathbf{x}}_n = \sum_{j=1}^J \omega_n^{(j)} \mathbf{x}_n^{(j)}.$$

For the considered estimation problem, the particle-based SPA is asymptotically optimum. This means that it can provide an approximation of the MMSE estimate in (6) that can be made arbitrarily good by choosing J sufficiently large [27]. For the processing of the *SWellEx-96* data we set $J = 10^4$.

IV. RAY TRACING

At each time step n , the proposed particle-based algorithm evaluates the nonlinear DOA function $g_k(\mathbf{p}_n)$ for each propagation path $k \in \{1, \dots, K\}$ a total of J times. DOAs are obtained by using BELLHOP [24] to calculate the eigenrays for the J source positions based on a SSP along the water column and the bathymetry information.

To reduce the runtime of the proposed algorithm, we precompute a 3-D matrix $\mathbf{Z} \in \mathbb{R}^{N_r \times N_d \times K}$ of DOAs that is used to interpolate the DOAs for each propagation path $k \in \{1, \dots, K\}$ and each source position $\mathbf{p}_n^{(j)}$, $j \in \{1, \dots, J\}$ during runtime.

The matrix \mathbf{Z} is obtained by performing the following steps:

- 1) we define a regular $N_r \times N_d$ grid of source positions $\mathbf{p}_n^{(i_r, i_d)}$, $i_r \in \{1, \dots, N_r\}$, $i_d \in \{1, \dots, N_d\}$ that covers the entire region of interest;
- 2) we use BELLHOP to calculate the eigenrays related to each source position on the grid $\mathbf{p}_n^{(i_r, i_d)}$, $i_r \in \{1, \dots, N_r\}$, $i_d \in \{1, \dots, N_d\}$ and select the K eigenrays that are expected to result in propagation paths for acoustic signals; and
- 3) we compute a 3-D matrix $\mathbf{Z} \in \mathbb{R}^{N_r \times N_d \times K}$ that consists of the DOAs of the K eigenrays at each of the $N_r \times N_d$ grid points; if eigenray $k \in \{1, \dots, K\}$ is geometrically impossible at a specific grid point, we set the corresponding element of matrix \mathbf{Z} to $-\infty$ and the corresponding detection probability $d_k(\mathbf{p}_n^{(i_r, i_d)})$ to zero.

For the processing of the *SWellEx-96* data we choose $N_r = 2400$ and $N_d = 165$, which correspond to a resolution of 1 m.

V. RESULTS

We validate the proposed method and compare it with matched field processing by using experimental data from a complex multi-path shallow-water environment [28], [29].

A. Setup of Experiment and DOA Estimation

Acoustic data sampled at 1500 Hz was recorded by a 64-element vertical linear array with a uniform inter-sensor spacing of 1.875 m that spanned water depths 94.125-212.25 m. The surface ship R/V Sproul traveled with a radial speed of 2.5 m/s towards the VLA with closest point of approach (CPA) at approximately 1 km. The ship towed an acoustic source at a depth of roughly 60 m that projects an acoustic signal that includes 13 tones at frequencies {49, 64, 79, 94, 112, 130, 148, 166, 201, 235, 283, 338, 388} Hz. The source track is shown in Fig. 1(a).

We process all 13 tones for the 20 minute interval indicated in Fig. 1(a). In particular, we perform beamforming by means of multifrequency sparse Bayesian learning (SBL) [20] as follows. First, the data are split into 1758 snapshots that consist of 2048 samples (1.37 s) and have 50 % overlap. For each snapshot a rectangular window is applied and a fast Fourier transform (FFT) is performed. The FFT length of 2048 samples corresponds to a bin width of 0.73 Hz. To accommodate Doppler shifts, for each of the 13 tones, we search the ± 1 FFT bins adjacent to the expected FFT bin and extract the FFT value with the maximum power. Next we perform multifrequency SBL for all tones and $L = 3$ consecutive snapshots. This results in 586 SBL solutions. Finally, we extract the DOA estimates from each SBL solution by finding (i) the 4 highest peaks and (ii) any additional peak that is within 35% of the highest peak. These DOA estimates are used as observations for the proposed method.

The SBL 586 solutions are shown in Fig. 4. In Fig. 4(a) and Fig. 4(b) expected DOAs related to the four dominate propagation paths are overlaid. These DOAs are obtained by using a source range calculate from the GPS system of the R/V Sproul, a reference depth of 60 m, and by applying the considered propagation model. In Fig. 4(b), the DOA estimates used as observations by the proposed method are highlighted in red. Note that around time 7 min and 11 min for an interval of approximately 74 s, the transmission of the 13 tones was interrupted. The 72 data segments corresponding to these time intervals were discarded, i.e., no DOA estimates were extracted. The remaining 514 data segments define the number of time steps of the proposed method.

B. System Parameters

We consider a region of interest of $[100\text{m}, 2500\text{m}] \times [10\text{m}, 175\text{m}]$ in range and depth. Source motion is modeled by assuming a nearly constant-velocity model [30] in range and a nearly constant-location model in depth, i.e.,

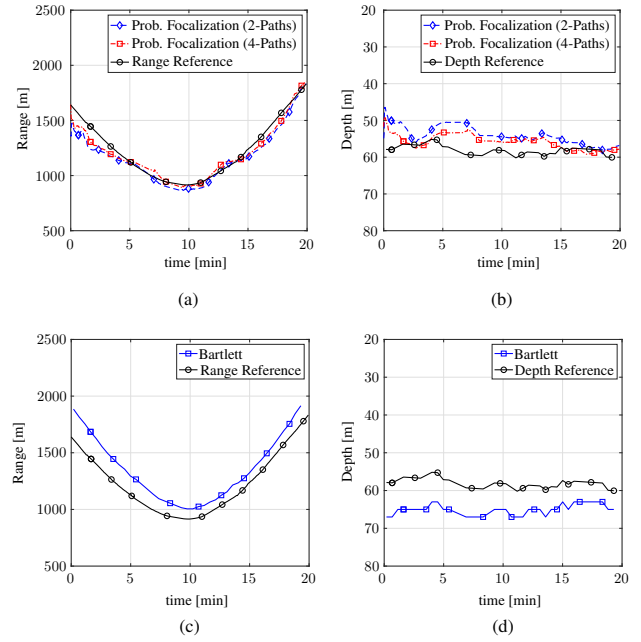


Fig. 5. Shallow water source localization results for the considered dataset from the *SWellEx-96* experiment. Probabilistic focalization results are shown in (a) & (b). MFP results are shown in (c) & (d). Compared to MFP, the proposed method is less sensitive to inaccurate bathymetry information.

$$\mathbf{x}_n = \begin{pmatrix} 1 & 0 & T_n \\ 0 & 1 & 0 \\ 0 & 0 & 1 \end{pmatrix} \mathbf{x}_{n-1} + \begin{pmatrix} \frac{T_n^2}{2} & 0 \\ 0 & T_n \\ T_n & 0 \end{pmatrix} \mathbf{u}_n \quad (8)$$

where \mathbf{u}_n is the driving noise and T_n is the length of the time step. If there is no data dropout, we have $T_n = 2.048\text{s}$. If data segments are missing, T_n is increased accordingly.

The driving noise $\mathbf{u}_n \sim \mathcal{N}(\mathbf{0}, \Sigma_u)$ with $\Sigma_u = \text{diag}\{0.05 \text{ m}^2/\text{s}^4, 0.1 \text{ m}^2/\text{s}^2\}$ is an independent and identically distributed (iid) sequence of 2D Gaussian random vectors. Note that (8) fully defines the state transition function $f(\mathbf{x}_n|\mathbf{x}_{n-1})$ discussed in Section II-A.

We process the DOA observations with the proposed method by considering the $K = 4$ propagation paths shown in Fig. 1. Furthermore, we also process the DOA observations by only considering the $K = 2$ propagation paths that are not affected by the seabed (DP and SB). Our model uses the SSP measured on the day of the event and shown in Fig. 1.

The observation noise standard deviations (cf. (1)) are set to $\sigma_k = 0.5^\circ$ for $k \in \{1, 2\}$ and $\sigma_k = 2^\circ$ for $k \in \{3, 4\}$. The larger standard deviation for the propagation paths that involve bottom bounces is motivated by the fact that constant bathymetry used by the model is inaccurate. The detection probabilities are set to $d_k(\mathbf{p}_n) = 0.9$ if propagation path k is geometrically possible and set to zero otherwise. The false alarm PDF $f_{\text{FA}}(z_{m,n})$ is uniform on $[-90^\circ, 90^\circ]$. The mean number of false alarms is $\mu_{\text{FA}} = 2$ for $K = 4$ and $\mu_{\text{FA}} = 4$ for $K = 2$. At time n , the prior distribution has the form $f(\mathbf{x}_0) = f(\mathbf{p}_0)f(v_0)$, where $f(\mathbf{p}_0)$ is uniform on $[100\text{m}, 2500\text{m}] \times [10\text{m}, 175\text{m}]$ and $f(v_0)$ is zero-mean Gaussian with standard deviation 5 m/s. Our implementation of the proposed method used $J = 10^4$ particles.

C. Performance Comparison

As a reference method, we consider MFP by means of the Bartlett processor. Both methods use the SSP, a constant bathymetry of 216.5 m, as well as the geo-acoustic parameters discussed in Ref. [8]. As a reference for the true range of the source, we use the heading and GPS position of the R/V Sproul and assume that the source is towed 100 m behind the vessel. As a reference for true source depth, we use the MFP solution compensated for bathymetry mismatch based on Eq. (10) in Ref. [28] and true seabed depths at the source locations.

Fig. 5 shows the shallow water source localization results for the considered 20 min of data. Range and depth estimation results for probabilistic focalization are shown in Fig. 5 (a) & (b). While only $K = 2$ propagation paths are needed for localization, using $K = 4$ instead of $K = 2$ propagation paths can slightly increase the range and depth estimation accuracy of the proposed method.

MFP results are shown in Fig. 5 (c) & (d). The range and depth bias of the MFP solution, also known as the mirage effect [28], is related to the fact that the assumed constant bathymetry is not accurate. In the considered scenario, the proposed method can outperform MFP despite relying on less environmental information. In particular, compared to MFP it is less sensitive to inaccurate bathymetry information. This is enabled by the proposed statistical model which makes it possible to assign different observation noise uncertainties to different propagation paths.

VI. CONCLUSION

We introduced a probabilistic focalization approach for the localization and tracking of an acoustic source in shallow water. Our method probabilistically associates observed DOAs to modeled DOAs and jointly estimates the time-varying source location. We demonstrated performance advantages compared to MFP using data collected during the *SWellEx-96* experiment. Notably, despite relying on less environmental information, the proposed method can outperform MFP in terms of range and depth estimation accuracy.

VII. ACKNOWLEDGEMENT

This research was supported by the Office of Naval Research under Grants N00014-21-1-2267 and N00014-21-WX-0-1634. We thank Prof. William S. Hodgkiss and Dr. Peter Gerstoft for helpful discussions.

REFERENCES

- [1] W. A. Kuperman, W. S. Hodgkiss, H.-C. Song, T. Akal, C. Ferla, and D. R. Jackson, "Phase conjugation in the ocean: Experimental demonstration of an acoustic time-reversal mirror," *J. Acoust. Soc. Am.*, vol. 103, no. 1, pp. 25–40, 1998.
- [2] M. J. Hinich, "Maximum-likelihood signal processing for a vertical array," *J. Acoust. Soc. Am.*, vol. 54, no. 2, pp. 499–503, 1973.
- [3] H. P. Bucker, "Use of calculated sound fields and matched-field detection to locate sound sources in shallow water," *J. Acoust. Soc. Am.*, vol. 59, no. 2, pp. 368–373, 1976.
- [4] A. B. Baggeroer, W. A. Kuperman, and P. N. Mikhalevsky, "An overview of matched field methods in ocean acoustics," *IEEE Journal of Oceanic Engineering*, vol. 18, no. 4, pp. 401–424, 1993.
- [5] M. D. Collins, L. T. Fialkowski, W. A. Kuperman, and J. S. Perkins, "The multivalued Bartlett processor and source tracking," *J. Acoust. Soc. Am.*, vol. 97, no. 1, pp. 235–241, 1995.
- [6] A. M. Thode, W. A. Kuperman, G. L. D'Spain, and W. S. Hodgkiss, "Localization using Bartlett matched-field processor sidelobes," *J. Acoust. Soc. Am.*, vol. 107, no. 1, pp. 278–286, 2000.
- [7] S.-H. Byun, C. M. A. Verlinden, and K. G. Sabra, "Blind deconvolution of shipping sources in an ocean waveguide," *J. Acoust. Soc. Am.*, vol. 141, no. 2, pp. 797–807, 2017.
- [8] K. L. Gemba, S. Nannuru, P. Gerstoft, and W. S. Hodgkiss, "Multi-frequency sparse Bayesian learning for robust matched field processing," *J. Acoust. Soc. Am.*, vol. 141, no. 5, pp. 3411–3420, 2017.
- [9] K. L. Gemba, W. S. Hodgkiss, and P. Gerstoft, "Adaptive and compressive matched field processing," *J. Acoust. Soc. Am.*, vol. 141, no. 1, pp. 92–103, 2017.
- [10] G. J. Orris, M. Nicholas, and J. S. Perkins, "The matched-phase coherent multi-frequency matched-field processor," *J. Acoust. Soc. Am.*, vol. 107, no. 5, pp. 2563–2575, 2000.
- [11] J. L. Krolik, "Matched-field minimum variance beamforming in a random ocean channel," *J. Acoust. Soc. Am.*, vol. 92, no. 3, pp. 1408–1419, 1992.
- [12] G. Byun, F. H. Akins, K. L. Gemba, H. C. Song, and W. A. Kuperman, "Multiple constraint matched field processing tolerant to array tilt mismatch," *J. Acoust. Soc. Am.*, vol. 147, no. 2, pp. 1231–1238, 2020.
- [13] F. Meyer, P. Braca, P. Willett, and F. Hlawatsch, "A scalable algorithm for tracking an unknown number of targets using multiple sensors," *IEEE Trans. Signal Process.*, vol. 65, no. 13, pp. 3478–3493, 2017.
- [14] F. Meyer, T. Kropfreiter, J. L. Williams, R. A. Lau, F. Hlawatsch, P. Braca, and M. Z. Win, "Message passing algorithms for scalable multitarget tracking," *Proc. IEEE*, vol. 106, no. 2, pp. 221–259, 2018.
- [15] E. Leitinger, F. Meyer, F. Hlawatsch, K. Witrissal, F. Tufvesson, and M. Z. Win, "A Belief Propagation Algorithm for Multipath-Based SLAM," *IEEE Trans. Wireless Commun.*, vol. 18, no. 11, pp. 5613–5629, 2019.
- [16] R. Mendrzik, F. Meyer, G. Bauch, and M. Z. Win, "Enabling situational awareness in millimeter wave massive MIMO systems," *IEEE J. Sel. Topics Signal Process.*, vol. 13, no. 5, pp. 1196–1211, 2019.
- [17] F. Meyer and M. Z. Win, "Scalable data association for extended object tracking," *IEEE Trans. Signal Inf. Process. Netw.*, vol. 6, pp. 491–507, May 2020.
- [18] F. Meyer and J. L. Williams, "Scalable detection and tracking of geometric extended objects," 2021, arXiv:2103.11279.
- [19] M. D. Collins and W. A. Kuperman, "Focalization: Environmental focusing and source localization," *J. Acoust. Soc. Am.*, vol. 90, no. 3, pp. 1410–1422, 1991.
- [20] S. Nannuru, K. L. Gemba, P. Gerstoft, W. S. Hodgkiss, and C. F. Mecklenbräuker, "Sparse Bayesian learning with multiple dictionaries," *Signal Process.*, vol. 159, pp. 159–170, 2019.
- [21] F. Meyer, Y. Park, and P. Gerstoft, "Variational Bayesian estimation of time-varying DOAs," in *Proc. FUSION-2020*, Pretoria, South Africa, 2020.
- [22] Y. Bar-Shalom, P. K. Willett, and X. Tian, *Tracking and Data Fusion: A Handbook of Algorithms*. Storrs, CT: Yaakov Bar-Shalom, 2011.
- [23] F. B. Jensen, W. A. Kuperman, M. B. Porter, and H. Schmidt, *Computational Ocean Acoustics*, 2nd ed. New York, NY: Springer, 2011.
- [24] M. B. Porter et al., "The Acoustics Toolbox," Online, 2020, available: <http://oalib.hlsresearch.com/AcousticsToolbox/>.
- [25] S. M. Kay, *Fundamentals of Statistical Signal Processing: Estimation Theory*. Upper Saddle River, NJ: Prentice-Hall, 1993.
- [26] F. R. Kschischang, B. J. Frey, and H.-A. Loeliger, "Factor graphs and the sum-product algorithm," *IEEE Trans. Inf. Theory*, vol. 47, no. 2, pp. 498–519, Feb. 2001.
- [27] M. S. Arulampalam, S. Maskell, N. Gordon, and T. Clapp, "A tutorial on particle filters for online nonlinear/non-Gaussian Bayesian tracking," *IEEE Trans. Signal Process.*, vol. 50, no. 2, pp. 174–188, 2002.
- [28] G. L. D'Spain, J. J. Murray, W. S. Hodgkiss, N. O. Booth, and P. W. Schey, "Mirages in shallow water matched field processing," *J. Acoust. Soc. Am.*, vol. 105, no. 6, pp. 3245–3265, 1999.
- [29] N. O. Booth, A. T. Abawi, P. W. Schey, and W. S. Hodgkiss, "Detectability of low-level broad-band signals using adaptive matched-field processing with vertical aperture arrays," *IEEE J. Ocean. Eng.*, vol. 25, no. 3, pp. 296–313, 2000.
- [30] Y. Bar-Shalom, T. Kirubarajan, and X.-R. Li, *Estimation with Applications to Tracking and Navigation*. New York, NY, USA: Wiley, 2002.